Annuaire de l'Université de Sofia "St. Kliment Ohridski", Faculté de Physique, 96, 2003

INFLUENCE OF THE DOPING ELEMENTS Sr, Zn, Mn, Gd ON CRYSTALLINE STRUCTURE, MECHANICAL AND MAGNETIC PROPERTIES OF DMS AND III–VI SEMICONDUCTORS

ZAHARI ZLATANOV

Department of General Physics

Захари Златанов. ВЛИЯНИЕ НА ЛЕГИРАЩИТЕ ЕЛЕМЕНТИ Sr, Zn, Mn, Gd ВЪРХУ КРИСТАЛНАТА СТРУКТУРА, МЕХАНИЧНИТЕ И МАГНИТНИТЕ СВОЙСТВА НА ПОЛУМАГНИТНИ ПОЛУПРОВОДНИЦИ ОТ СИСТЕМАТА III–IV

В настоящата работа е направен обзор на проблемите, свързани с получаването на монофазни кристали и влиянието на различни легиращи елементи върху кристалната структура и създаването на дефекти в получените материали. Направен е преглед на получените през последните няколко години експериментални резултати от изследване на влиянието на примесните атоми върху микротвърдостта и магнитните своиства. Изследвано е влиянието на различни видове дефекти, като ваканции и примесни атоми, върху кристалната структура. Изследваните материали са полумагнитни полупроводници, полупроводникови сплави и системи $A_{1-x}B_xC$, легирани със Sr, Zn, Mn, Gd. Образците са монокристали, тънки слоеве и хетероструктури, получени чрез метода на Бриджман, молекулно-лъчева епитаксия, пряк синтез. Направен е преглед на различни модели и методи за изследване на влиянието на концетрацията на примесните елементи и тяхното положение в основната кристална решетка върху структурните параметри и магнитните им свойства.

Zahari Zlatanov. INFLUENCE OF THE DOPING ELEMENTS Sr, Zn, Mn, Gd ON CRYSTALLINE STRUCTURE, MECHANICAL AND MAGNETIC PROPERTIES OF DMS AND III-VI SEMICONDUCTORS

In this work, we present the problems associated with preparing of single phase crystals, and influence of doping elements on microstructure and creating of defects into materials. The experimental results from recent studies of microhardness and magnetic properties are shown. The influence of defects, as vacancies and impurity atoms on structural parameters is investigated. The materials are DMS, semiconductor alloys and $A_{1-x}B_xC$ systems (with B = Sr, Zn, Mn, Gd). They are layers, heterostructures and monocrystals obtained by Bridgeman method, MBE, and direct synthesis. Here different models and methods are presented for investigation of the dependence of structural parameters and magnetic properties on doping element concentration, and impurity ion sites into host lattice.

Keywords: defects and impurities in crystals, microstructure

PACS number: 61.72-Y

INTRODUCTION

Dilute magnetic semiconductors (DMS) are semiconductor alloys whose lattices are made up in part of substitutional magnetic atoms. Due to their unique magnetic, magnetooptical, electrical, and optical properties, DMS have attracted a great deal of attention. For example, the energy gap and lattice parameter can be tuned by changing the composition. Because of the exchange interactions between local magnetic moments and band electrons, many interesting phenomena have been discovered, such as extremely large Faraday rotation, giant negative magnetoresistance, and the magnetic polaron.

Besides, under the external magnetic field, the properties of spin-glass transition, antiferromagnetic interaction, and magnon excitation have been observed.

DATA, METHODS AND MODELS

For materials of interest in a group of compounds described as semimagnetic semiconductors (SMSC) the majority of studies have been on chalcogenides of lead, tin. germanium, or cadmium containing manganese as the magnetic species (PbTe, SnTe, GeTe, CdTe⟨Mn⟩, PbTe⟨Gd⟩)

Among the studies of DMS, the reports of Mn-based DMS are abundant. In these materials, the presence of substitutional Mn^{2+} ions carrying a bare spin of 5/2 is responsible for the magnetic properties [1–3].

The $Cd_{1-x}Mn_xTe$ alloys are the most extensively studied and probably best understood of the wide-gap DMS.

In the case of Zn-doped materials $Cd_{1-x}Mn_xTe$, it is interesting that a Debye-like relaxation has been observed, which is attributed to the electron hopping among crystal defects. The relaxation is found to be thermally activated, and the obtained activation energy decreases with increasing Zn content. It is found that the energy gap of this alloy system can be tuned from 1.6 to 2.7 eV at 10 K. It thus provides a potential candidate for the application of optoelectronic devices in the infrared and visible region.

An other alloy system with application in infrared region is the narrow-gap $Pb_{1-x}Gd_xTe$ antiferromagnetic material with energy-gap at room temperature 320 meV (for investigated content of gadolinium $x < 0.1$).

In the present work, the $Pb_{1-x}Gd_xTe$ alloys with nominal values of x (0.001–0.2) were prepared by the Bridgeman method or horizontal Bridgeman method. Both X-ray diffraction and microprobing indicated a single phase for alloys with $x < 0.1$.

From X-ray powder refractograms NaCl-type structure is confirmed NaCl-type structure and lattice parameter $a = 6.46$ Å, single phase, good solubility of impurity into host lattice. Here is too high vapour pressure of Te. Experimentally registered strong influence of gadolinium on microhardness—at higher impurity

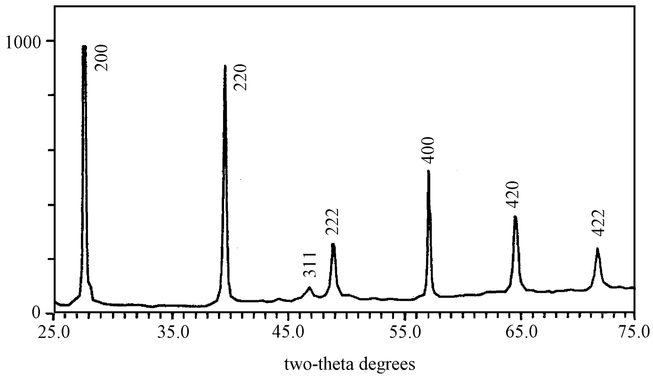

Fig. 1. X-ray powder diffractograme of sample $Pb_{1-x}Gd_xTe$ at $x = 0.05$ (here not change of lattice constant a of PbTe)

concentrations Fig. 2. There is observed also a dependence—concentration of cation vacancies on concentration of rare-earth atoms.

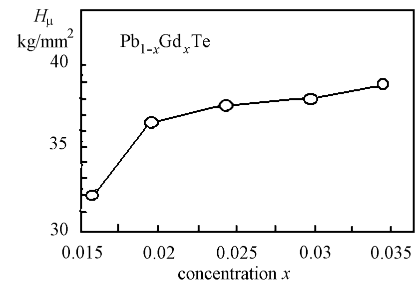

Fig. 2. Dependence: microhardness H_μ versus impurity concentration x (sample with x from 0.005 to 0.05)

In the last years investigations were made on the magnetic effects due to introducing La-element Gadolinium into the semiconductor PbTe. These results were compared (experimental data from magnetic measurements) with the earlier works on manganese in the same host [4]. The majority of reported results are from measurements on the temperature and concentration dependence of the low-field ac-susceptibility and preliminary electron paramagnetic resonance (EPR) results on $Pb_{1-x}Gd_xTe$ alloys in the temperature range from room temperature to liquid helium. EPR and low-field ac-susceptibility measurements were done on the rare- earth doped semimagnetic semiconductor $Pb_{1-x}Gd_xTe$ for the Gd composition range $x = 0.001$ to 0.02. For the lower concentrations, the EPR results indicate a fully resolved fine-structure lines appropriate to the Gd^{3+} ions (Gd spin of 7/2 in cubic symmetry host lattice).

Deviations from this simple behaviour are observed for Gd concentrations greater that $x \gg 0.05$ and for $T < 10$ K. Evidence is observed for an antiferromagnetic clustering of impurity spins. If one assumes clusters formed by pairs of spins coupled antiferromagnetically, then the susceptibility results can be used to give an estimate of the number of spins that have formed clusters.

For materials as the cobaltites: $LaCoO_3$ and doping $Sr(x)$ materials, $La_{1-x}Sr_xCoO_3$, the electronic structure has been obtained as a function of Sr substitution. The energetics of different spin configurations are estimated using the fixed-spin-moment (FSM) method.

It has been reported that the La_{1-x} Sr_xCoO_3 phase develops a ferromagnetic long-range order above $x = 0.05$ and that the metal–insulator transition takes place at $x \sim 0.2$ [5].

Optical measurements show that the electronic structure of the high-temperature metallic state of $LaCoO_3$ is very similar to that of the doping-induced metallic state. Hence, the FSM calculations on hole-doped $LaCoO_3$ are expected to give a better understanding about the nature of the temperature-induced spin-state transition.

The magnetic properties of the cobaltites depend on the spin state of Co^{3+} and Co^{4+}, i.e. whether they are in the low (LS), intermediate (IS) or high-spin (HS) state. From photoemission measurements it has been conclude that the hybridisation of oxygen 2p orbitals and cobalt 3d states stabilises the IS state with spin $S = 1$ [6].

To study spin fluctuations it is advantageous to calculate the total energy as a function of magnetic moment using the so-called fixed-spin-moment method [7, 8]. In this method one uses the magnetic moment M as an external parameter and calculates the total energy as a function of M. In general one must release the constraint that the Fermi levels for up and down spins are equal because the equilibrium condition is not satisfied for arbitrary M. The number of valence electrons N is known and M is fixed determining the values for $E_F \uparrow$ and $E_F \downarrow$.

For the Sr-doped system, it is natural that the Sr substitution induces a partial oxidation from Co^{3+} to Co^{4+}. From the effective magnetic moment obtained by magnetisation measurements, Taguch and Shimada [9] concluded that Co^{3+} is in an HS state in $La_{1-x}Sr_xCoO_3$ and Co^{4+} in an LS state because the saturation moment in the ferromagnetic phase $(0.3 > x)$ is only about half the full moment of HS Co^{3+}.

A transition from LS to HS through doping has been suggested from NMR studies [10] on ^{59}Co and ^{139}La probes and neutron scattering [11]. Electron spectroscopy [12] and magnetic measurements indicate [5, 13] that hole doping leads to the formation of HS rather than LS configuration. As the radius of Sr^{2+} is larger than that of La^{3+}, it is suggested that the Sr doping favours the HS state by the introduction of Co^{4+} $(3d^5)$.

Hence, the calculated magnetic moments are always smaller than the ionic values, and much smaller than the HS ionic value indicating that this discrepancy cannot be accounted for as a hybridisation effect. It should be noted that one can expect a discrepancy between experiment and theory above $x > 0.5$, where the oxygen deficiency is known to increase significantly.

In the case of substitution into host lattice, the hole-doping effect in $LaCoO^3$ has been simulated using supercell calculations as well as VCA calculations. For the VCA calculation we have taken into account the experimentally reported structural parameter changes as a function of Sr substitution. Hence, these calculations accounted properly for the hybridisation effect. In this approximation the true atom in the material is replaced by an "average" atom which is interpolated linearly in charge between the corresponding pure atoms. In the VCA calculations the charge-transfer effect is not thoroughly accounted for, whereas the band-filling effects are properly taken into account. The chosen approximation has an advantage owing to its simplicity and hence we are able to study small concentrations of Sr in $LaCoO^3$. However, for 50% Sr substitution we have made explicit supercell FSM calculations.

Consequently, in other case, from magnetic measurements data, using this method (FSM) and obtaining electron-structure can been confirmed substitution state on doping magnetic ions into crystal structure.

The alloys, $Cd_{1-x-y}Zn_xMn_yTe$, were grown by temperature gradient solution growth with the temperature gradient close to 50° C/cm. The tellurium element was used as solvent, the anion (Te^{2-}) to cation (Cd^{2+}, Zn^{2+}, Mn^{2+}) molar ratio was 7 to 3. The large temperature gradient enables the impurities and excess Te to segregate to the higher temperature region. The crystal structure has been checked by X-ray measurement. The composition has been determined by energy dispersive X-ray spectroscopy (EDAXS) analyse. For all the crystals studied here, the Mn concentration is fixed at $x = 0.05$. The Zn composition is scanned from 0 to 0.95. The optical properties of the crystals have been studied by photoluminescence and reflectivity measurements.

If here has considered the dependence of the activation energy on Zn content, it is can clearly see that the magnitude of the activation energy decreases with the increase of Zn concentration in a monotonous way (The activation energy (E) is the energy for carrier hopping as a function of Zn concentration x; the Mn concentration in the material studied $y = 0.05$ is fixed).

To interpret this result we can use the four-center model, first suggested in [14]. A microscopic structure of the defects based on the four-center model is proposed to explain the observed behaviour.

Considering an alloy $A_{1-x}B_xC$ with a zinc-blende structure, we assume the defect center locates at the C vacancy. If the defect wave function is sufficiently localised, the defect center is confined to the C vacancy and its nearest neighbours. There are four kinds of configurations of nearest-neighbour sites occupied by A or B atoms—four-center model of the structure of the defect D, which locates at a site in the C sublattice. As the concentration of B atoms increases, the number of B atoms near the C vacancy increases. Because the configurations of the nearest-neighbors of defects change with the increase of B atoms, the behaviour of defect is thus changed.

This behaviour is attributed to the charge redistribution by carrier hopping among defects. The variation of the activation energy of carrier hopping with Zn concentration is monotonic. This result is described by means of the four-center model, in which the number of Zn atoms appearing in the nearest-neighbor sites of a defect can have four possible configurations.

For $Cd_{1-x-y}Zn_xMn_yTe$ alloys, can neglect the effect of the Mn atom because its concentration is fixed at a small value of 0.05. Therefore the Four-center model of the structure of the defects that differ with respect to the number of Zn atoms appearing in them is used to account for the variation of activation energies. Because the number of Zn atoms appearing in the neighbors of the defect changes discretely, the properties of the defect should also reflect the same behaviour. The similar defect behaviours has also been observed in ZnCdTe by deep-level transient spectroscopy [15]. The evidence of the four-center model have been observed in many alloy, such as GaAsP [16], GaInP [17], and ZnSSe.

An other material, which has been studied intensively during last years is La-doped $PbTiO_3$. Here, the effect of La-doping leads to cubic-tetragonal phase transition and short-range ordering.

It is well known that La^{3+} ion (r = 1.032 Å) replaces Pb^{2+} ion (r = 1.19 Å) rather than Ti^{4+} ion (r = 0.605 Å) in Pb-based material. When La^{3+} ion is substituted for Pb^{2+} ion, the charge compensation is essential. If the A site (Pb site) is compensated, one vacant site is created by the substitution of two La^{3+} ions. Let us call this system the PLT-A.

On the other hand, if the B site (Ti site) is compensated, one vacant site is produced on the B-site sublattice by four La^{3+} ions. Let us call this system the PLT-B. Considering a coexistence of these two distinct types of vacancies at a given thermodynamic condition, one can represent the stoichiometry of PLT.

Typical normal ferroelectrics such as $PbTiO_3$ are known to exhibit the relaxor ferroelectricity under a suitable doping condition (or here is observed transition normal-to-relaxor ferroelectrisity). In the case La-doped element, for example, La-modified $PbTiO_3$ in the tetragonal phase field with transition from a normal ferroelectric state to a relaxor state for the La content higher than 12 at.% [18].

These observations can be used to better understand the origin and the atomistic mechanism responsible for the manifestation of relaxor ferroelectrisity in terms of the nature of site defects introduced by the doping. When it is modified by La^{3+} ions, cation vacancies are created to keep the charge neutrality, producing a mixture of two distinct vacant sites (this model can be applied to other materials—PbTe for example, where: A site (Pb site) and B site (Ti site) vacancies).

Recently, a simple processing route was developed that suitably adjusts the relative concentration of these two distinct cation-site vacancies. Using this processing scheme, it was shown that the microscopic inhomogeneity caused by the B-site vacancy is primarily responsible for the manifestation of relaxor behaviour from normal ferroelectricity in La-modified $PbTiO_3$ [19].

The main purpose of many studies is to experimentaly examine the effects of these two distinct cation-site (A/B) vacancies on: (1) the characteristics of structural cubic-tetragonal transitions, and (2) the formation and growth of the short-ranged clusters with tetragonal symmetry in the high-temperature cubic-phase field of $PbTiO_3$. Effects of cation-site vacancies on the characteristics of the cubic-tetragonal displacive transitions in La-modified $PbTiO_3$ (PLT) were studied using in XRD measurements and Raman scattering. For this purpose, two distinct types of PLT series having cation-site vacancies either at the A site or at the B site were separately prepared. The PLT-A series exhibited under went the cubic to tetragonal structural transition for La substitution up to 30 at.%. Contrary to this, the PLT-B became with the absence of the macroscopic cubic to tetragonal transition.

These observations were attributed to the formation of short-ranged clusters with tetragonal symmetry in a globally cubic matrix and to the reduced dipolar interaction between the clusters in the PLT-B, as compared with the PLT-A.

Binary chalcogenide alloys of the type III_2–VI_3, with group VI: elements S, Se, and Te have been widely studied during the last decade and the potential application of In_2Se_3 as an absorber material in a photovoltaic cell has revived interest in this compound.

The problems associated with preparing single-phase crystals, are the many different crystalline phases that exist for In_2Se_3, the numerous other In-Se compounds as well as the high vapour pressure of Se. The large influence that the microstructure and secondary phases (surface layers) may have on the transport properties contributes further to the confusion. The possibility for obtaining of sublattice from magnetic ions is used in the case of heteroepitaxy, i.e. growth of 2D layers and formation of 3D structure into semiconductor host lattice.

Layered III–VI semiconductor compounds have long been studied due to the fundamental interest in the unusual nature of electronic interactions present in such compounds and also due to their potential application in non-linear optics [20], solar cells, and solid state batteries [21]. The recent observation of the Van der Waals-like epitaxy between two-dimensional (2D) lamellar semiconductors [22, 23] led to the hope that conventional three-dimensional (3D) semiconductors could achieve heteroepitaxy by means of the insertion of a few 2D layers in between the semiconductors [24–29].

The capacity of layered structures to accommodate strong lattice mismatches could help to achieve a good epitaxy. Fabrication of high-quality bulk InSe and GaSe crystals in the form of plate lets was accomplished using the Bridgman technique. Samples were cut into parallelepipeds.

Phase identification and crystallographic orientation were accomplished with selected area electron diffraction (SAED) in transmission electron microscopy (TEM) (as EDAX in scanning electron microscopy-SEM), CoKa X-ray diffraction (XRD) in the $\theta - 2\theta$ geometry.

The determination of hardness and elastic modules of the samples employs the Oliver and Pharr methodology [30], which calculates these properties from the load-displacement data. A Berkovich diamond tip with an inverse triangular pyramidal shape (faces 65.3° from vertical axis) was used in the tests.

Angular dependence of the hardness is clearly observed for InSe and GaSe. The plastic deformation induced in a crystal after application of a definite shear stress can be effected either by slip or by twinning. These processes do not take place simultaneously over all crystallographic planes and orientations, but successively involve the planes and directions which are oriented most favourably relative to the direction of the stress field and in which the shear stress increases to the critical value necessary to activate the slip and twinning. Slip and twinning processes are anisotropic, i.e. the displacement of atomic layers takes place only along particular crystallographic planes and directions.

Thus, the angular dependence of the measured hardness showing minimal values coinciding with the preferential slip directions could be reasonably understood in terms of the slip process between lamellar sheets. The similarity between the geometry of the Berkovich tip and threefold coordination for Se and X (In or Ga) atoms favours a symmetrical rupture of the bonds in Se–X and X–Se sublayers. Due to the hexagonal atomic planes of Se, the easy slip, which is expected between lamellar sheets, occurs along the same easy slip directions of the hexagonal crystals. The amplitude of the angular variation of the hardness of our samples is around 12 % and 14.5 % of the average hardness values for InSe and GaSe, respectively.

The measured hardness decreases with increasing loads in both materials. This is probably related to the fact that the plastic deformation is dominated by pop-in events. At high loads and penetrations the tip displacement during a single pop-in event tends to be higher than at low loads.

InSe and GaSe are lamellar compounds which can be described by a stacking sequence of sheets along the [001] direction where each sheet consists of four atomic planes Se–X–X–Se (X = In, Ga). The atoms within a sheet are bonded through ionocovalent forces, whereas the sheets are held together via weak van der Wals-like forces. All bonds are confined within the sheets with surfaces terminated by Se atoms and arranged in a sixfold triangular lattice with a common parameter a equal to 4.00 Åand 3.74 Åfor InSe and GaSe, respectively. The unit cells are hexagonal with a lattice constant a.

The 2D structure of the unit sheet formed by two hexagonal atomic planes (Se–X with X = In or Ga) with metallic and selenium atoms at alternate corners of the hexagons is clearly observed. According to the load versus displacement measurements with materials (monocrystals) a progressive plastic deformation occurs above 100 mN of load [28]. The In–In bond presumably weakenes under pressure and is subsequently broken. A fraction of In atoms from each layer jump to the interlayer space and the Se–In–In–Se plane sequence changes to a Se–In–Se–In sequence in a transition toward a NaCl-type structure.

Lead telluride is a IV–VI semiconductor compounds with rocksalt structure Fig. 3. Gadolinium, which is a $4f^7$ rare-earth magnetic ion, was introduced in the lattice host PbTe to obtain $Pb_{1-x}Gd_xTe$ semimagnetic semiconductor (SMSC). The aim of few works is to study the exchange effect between Gd ions in this structure. Previous magnetic studies [31] on these alloys, showed a small negative Curie temperature θ, and did not reveal long-range magnetic ordering even in high-concentration samples up to $x = 0.45$.

In the case of $Pb_{1-x}Gd_xTe$, with lower concentration $x \ll 0.05$ is supposed formation of sublattices from magnetic ions Gd^{3+} (Fig. 4) with different type of crystal symmetry (cubic, or tetragonal), which corresponding to nearest-neighbor (NN) Fig. 5a or next nearest-neigbor (NNN) Fig. 5b magnetic ions orderng re-

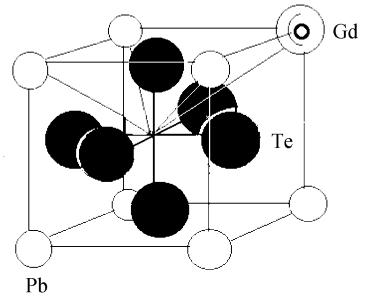

Fig. 3. Unit cell of PbTe monocrystalline (with NaCl type lattice). Gd-atom as substitution's ion on cation site

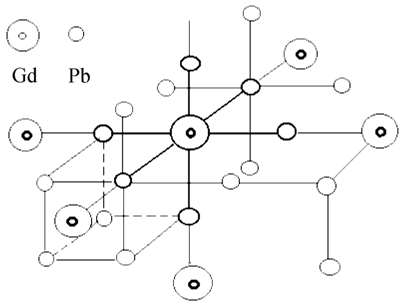

Fig. 4. Monocrystalline lattice of PbTe⟨Gd⟩ (impurity rare-earth ion ordering into cation-lattice)

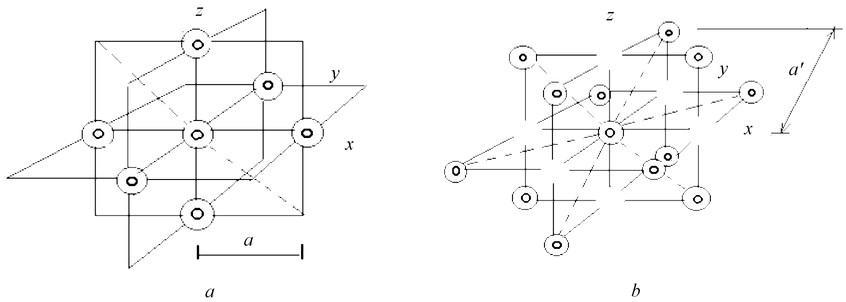

Fig. 5. Impurity atom site into host lattice PbTe: (*a*) Gd-atom at coordination number $z = 6$; (*b*) Gd-atom at coordination number $z = 12$

spectively. From microhardness measurements of monocristalline samples with single-phase, there is observed impurity concentration x dependence Fig. 2. In order to interprete experimental data (H_μ/x) a possible formation of short-range magnetic-ion clusters was assumed at high concentration $(x > 0.05)$ and sublattice at lower concentrations $(x < 0.05)$ in the host cubic matrix PbTe (Fig. 6).

In the range $0 < x < 0.05$, the microhardness depends both on impurity concentration (H_μ/x), and the ratio between cation-vacancies concentration $(C\ \%)$ and number of impurity atoms Gd (N_d) (i.e. C/N_d into the host lattice), as there is random impurity distribution into cation-sites if $C \gg N_d$. At x values about and above $x > 0.005$ sublattice from magnetic ions is formed which could be considered as ordered magnetic ions, which substitute part of Pb atoms into cation lattice. In this case from experimental data an increase is observed of H_μ (in the case $C < N_d$).

From magnetic susceptibility one can estimate the coordination number z of magnetic ions as a function of impurity concentration x into host lattice, as it is the case of antiferomagnetic material $Pb_{1-x}Gd_xTe$.

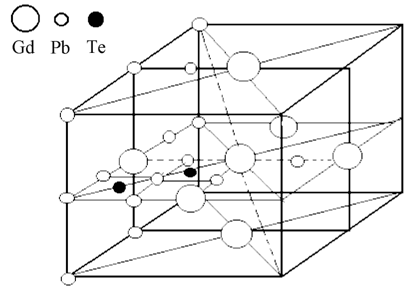

Fig. 6. Formation of magnetic-ion sublattice in the case of $z = 6$ and NNN exchange interaction

In some previous papers, experimental data were reported on magnetic susceptibility and magnetisation of $Pb_{1-x}Gd_xTe$ [32, 33]. The data have been explained by taking into account isolated rare-earth ions and pairs with contributions from larger clusters being early negligible for the small values of x that were investigated. The nearest-neighbor (NN) exchange interactions that were obtained were quite small, similar to those in other IV–VI DMS with the NaCl structure.

Both the susceptibility and the high-field magnetisation data indicated a weak antiferromagnetic coupling among Gd ions. There is a dependence of the exchange interaction of Gd ions on cation-anion separation in the NaCl-type lattice. Also, there is a possibility of a indirect exchange interaction via free carriers in DMS with high carrier concentration. Such effects have been observed in $Sn_{1-x}Mn_xTe$ [34–36].

In the Gd compounds the next-nearest-neighbor (NNN) interaction parameter J is claimed to be bigger than the nearest-neighbor (NN) interaction parameter J_{NN}. There is evidence of magnetic-ion ordering. In the Gd chalcogenides the NN exchange is claimed to be antiferomagnetic, and NNN exchange is also antiferomagnetic (except EuS) [37]. As a consequence of the (rocksalt) structure of these compounds, a dominant exchange interaction can be proposed exerted between next-nearest-neighbor ions. But there is a dependence of x/NN (or NNN).

Consequently, here a dependence should exists between doping concentration x of magnetic ions, value of exchange interaction J, and position of ions into host lattice. According by these positions should form a magnetic-ion sublattice, with a lattice parameter and coordination number z_1 and z_2 of NN and NNN respectively, on cation sites. In the case of monocrystalline samples, with $C_{\min}$ of cation-vacancies, also there should be a dependence between concentration of Gd ions and free carrier concentration. Hence, from magnetic measurements and experimental data on H_m and X-ray diffractograms, one can conclude about NN or NNN ordering (Fig. 5*a*, Fig. 5*b*) and formation of impurity-ion sublattice (Fig. 6)

CONCLUSIONS

Results for materials as Se–X (X = In, Ga) indicate that nanoindentation experiments can be used to check certain theoretical assumptions about mechanical behaviour and change of structural properties.

Measurements of the anisotropic hardness indicate that the slip process between lamellar sheets (for III–VI semiconductors) is the predominant mechanism of deformation in these crystals. Direct calculations are in good agreement with the measured H_μ and previous experimental values.

These observations can be used to better understand the origin and the atomistic mechanism responsible for the manifestation in terms of the nature of site defects introduced by the doping.

When it is modified by La^{3+} ions (predominantly about La-SMSC), cation vacancies are created to keep the charge neutrality, producing a mixture of two distinct vacant sites: A-site (Pb-site) and B-site (Ti-site) vacancies.

These observations were attributed to the formationof short-ranged clusters with tetragonal symmetry in a globally cubic matrix.

In the case of $Pb_{1-x}Gd_xTe$ SMSC, there is possibility for substitution on cations (Pb sites) from magnetic ions Gd and formation (at lower concentrations $x \ll 0.05$) of sublattice with different, from host lattice, unit-cell structure.

REFERENCES

1. Cocharane, R. W., M. Plischk, J. Strom - Olsen. *Phys. Rev. B*, **9**, 1973, 3013.
2. Gaz, J. A., R. R. Galazka, M. Nawrochi. *Solid State Commun.* **23**, 1977, 894.
3. Oseroff, S., F. Acker. *Solid State Commun.*, **7**, 1980, 19.
4. Escorne, M., A. Mauger, J. L. Tholence, R. Triboulet. *Phys. Rev. B*, **29**, 1984, 6306.
5. Jonker, G. H., J. H. van Santen. *Physica (Amsterdam)*, **19**, 1953, 120.
6. Potze, R. H., G. A. Sawatzky, M. Abbate. *Phys. Rev. B*, **51**, 1995, 11501.
7. Williams, A. R., V. L. Moruzzi, J. Kubler, K. Schwarz. *Bull. Am. Phys. Soc.*, **29**, 1984, 278.
8. Moruzzi, V. L., P. M. Marcus, K. Schwarz, P. Mohm. *Phys. Rev. B*, **34**, 1986, 1784.
9. Taguchi, H., M. Shimada, M. Koizum. *Mater. Res. Bull.*, **13**, 1978, 1235.
10. Itoh, M., I. Natozi. *J. Magn. Magn. Mater.*, **140-144**, 1995, 2145.
11. Asai, K., O. Yokokura, N. Nishimori, H. Chou, J. M. Tranquada, G. Shirane, S. Higuchi, Y. Okajima, K. Kohn. *Phys. Rev. B*, **50**, 1994, 3025.
12. Chainani, A., M. Mathur, D. D. Sarma. *Phys. Rev. B*, **46**, 1992, 9976.
13. Raccah, P. M., J. B. Goodenough. *J. Appl. Phys.*, **39**, 1968, 1209.
14. Fonger, W. H. *Phys. Rev.*, **137**, 1965, A1038.
15. Zerrai, A., G. Marrakchi, G. Bremond. *J. Appl. Phys.*, **87**, 2000, 4293.
16. Samuelson, J., S. Nillsson, Z. G. Wang, H. G. Grimmeisss. *Phy. Rev. Lett.*, **53**, 1984, 1501.
17. Zunger, A. *Phys. Rev. Lett.*, **54**, 1985, 849.
18. Dai, X., A. D. Giovanni, D. Viehland. *J. Appl. Pys.*, **74**, 1993, 3399.
19. Kim, T. Y., H. M. Jang. *Appl. Phys. Lett.*, **77**, 2000, 3824.
20. Amzallag, J., H. Benisty, S. Debrus, M. May, M. Eddrief, A. Bourdon, A. Chevy, N. Picciolly. *Appl. Phys. Lett.*, **66**, 1995, 982.
21. Gomes da Costa, P., M. Balkanski, R. F. Wallis. *Phys. Rev. B*, **43**, 1991, 7066.
22. Oshusi, F. S., T. Shimada, B. A. Parkinson, K. Ueno, A. Koma. *J. Cryst. Growth*, **111**, 1991, 1033.
23. Emery, J. Y., L. Brahim-Ostmane, C. Hirlimann, A. Chevy. *J. Apll. Phys.*, **71**, 1992, 3256.
24. Ueno, K., H. Abe, K. Saiki, A. Koma. *Jpn. J. Appl. Phys.*, Part 2, **30**, 1991, L352.
25. Thanh Vinh, L., M. Eddrief, C. Sebenne, A. Sacuto, M. Balkanski. *J. Cryst. Growth*, **135**, 1994, 1.
26. Thanh Vinh, L. M. Eddrief, J. E. Mahan, A. Vantomme, J. H. Song, M. A. Nicolet. *J. Appl. Phys*, **81**, 1997, 7289.
27. Koebel, A., Y. Zheng, J. F. Petroff, J. C. Boulliard, B. Capelle, M. Eddrief. *Phys. Rev. B*, **56**, 1997, 12296.

28. Jedrecy, N., R. Pinchaux, M. Eddrief. *Phys. Rev. B*, **56**, 1997, 9583.
29. Palmer, J., T. Saitoh, T. Yodo, M. Tamura. *J. Cryst. Growth*, **147**, 1995, 283.
30. Oliver, W. C., G. M. Pharr. *J. Mater. Res.*, **10**, 1992, 1564.
31. Savage, H. T., J. J. Rhyne. *Magnetism and Magnetic Materials* – 1971 (Chicago) Proceedings of 17th Annual Conference, p. 879
32. Gorska, M., J. R. Anderson, Z. Golacki. In SMSC (Materials research society, Pittsburgh, 1987), p.119.
33. Anderson, J. R., G. Kido, Y. Nishina, M. Gorska, L. Kowalczyk, Z. Golacki. *Phys. Rev. B*, **41**, 1990, 1014.
34. Mathur, M. P., D. W.Deis, C. K. Jones, A. Patterson, W. J. Carr, R.C. Miller. *J. Appl. Phys.*, **41**, 1970, 1005.
35. Mauger, A., M. Escorne. *Phys. Rev. B*, **35**, 1987, 1902.
36. Jonge, W. J. M. de, H. J. M. Swagten, S. J. E. A. Eltink, N. M. J. Stoffels. In: *Narrow-gap Semicinductors and Related Materials*, Proceedings of the International Conference on Narrow-gap semiconductors an Relate Materials (IOP, Bristol, England 1990).
37. Mc Guire, T. R., R. J. Gambino, S. J. Pickart, H. A. Alperin. *J. Appl. Phys.*, **40**, 1969, 1009.

Zahari Zlatanov
St. Kliment Ohridski University of Sofia
Faculty of Physics
Department of General Physics
5 James Bourchier Blvd.
BG-1164 Sofia, Bulgaria
E-mail: zlatanov@phys.uni-sofia.bg

Received April 2003